9

Rolling contact of inelastic bodies

9.1 Elastic hysteresis

No solid is perfectly elastic. During a cycle of loading and unloading even within the so-called elastic limit some energy is dissipated. The energy loss is usually expressed as a fraction α of the maximum elastic strain energy stored in the solid during the cycle where α is referred to as the 'hysteresis loss factor'. For most metals stressed within the elastic limit the value of α is very small, usually less than 1%, but for polymers and rubber it may be much larger.

The material of bodies in freely rolling contact undergoes a cycle of loading and unloading as it flows through the region of contact deformation (see Fig. 9.1). The strain energy of material elements increases up to the centre-plane ($x = 0$) due to the work of compression done by the contact pressure acting on the front half of the contact area. After the centre-plane the strain energy

Fig. 9.1. Deformation in rolling contact. An element of material experiences the cycle of reversed shear and compression *A–B–C–D–E*.

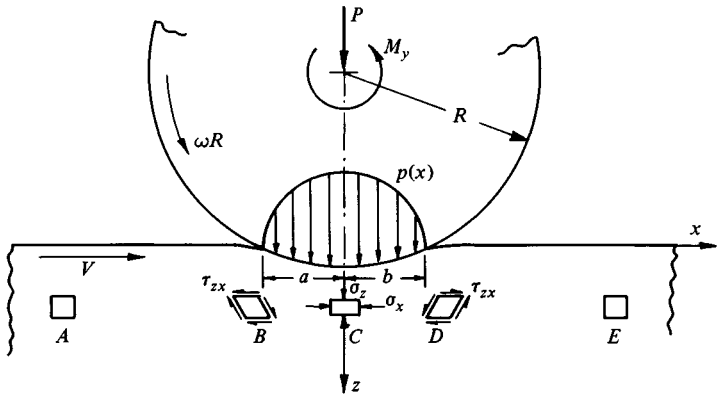

https://doi.org/10.1017/CBO9781139171731.010 Published online by Cambridge University Press

decreases and work is done against the contact pressure at the back of the contact. Neglecting any interfacial friction the strain energy of the material arriving at the centre plane in time dt can be found from the work done by the pressure on the leading half of the contact. For a cylindrical contact of unit width

$$\mathrm{d}W = \omega \, \mathrm{d}t \int_0^a p(x)x \, \mathrm{d}x$$

where $\omega (= V/R)$ is the angular velocity of the roller. Taking $p(x)$ to be given by the Hertz theory

$$\dot{W} = \frac{2}{3\pi} Pa\omega \tag{9.1}$$

where P is the contact load. If a small fraction α of this strain energy is now assumed to be dissipated by hysteresis, the resultant moment required to maintain the motion is given by equating the net work done to the energy dissipated, then

$$M_y \omega = \alpha \dot{W} = \frac{2}{3\pi} \alpha Pa\omega$$

or

$$\mu_R \equiv \frac{M_y}{PR} = \alpha \frac{2a}{3\pi R} \tag{9.2}$$

where μ_R is defined as the coefficient of rolling resistance. Thus the resistance to rolling of bodies of imperfectly elastic material can be expressed in terms of their hysteresis loss factor. This simple theory of 'rolling friction' is due to Tabor (1955).† Performing the same calculation for an elliptical (or circular) contact area gives the result.

$$\mu_R \equiv \frac{M_y}{PR} = \alpha \tfrac{3}{16} \frac{a}{R} \tag{9.3}$$

where a is the half-width of the contact ellipse in the direction of rolling. For a sphere rolling on a plane, a is proportional to $(PR)^{1/3}$ so that the effective rolling resistance $F_R = M_y/R$ should be proportional to $P^{4/3}R^{-2/3}$. This relationship is reasonably well supported by experiments with rubber (Greenwood *et al.*, 1961) but less well with metals (Tabor, 1955).

The drawback to this simple theory is twofold. First, the hysteresis loss factor α is not generally a material constant. For metals it increases with strain (a/R), particularly as the elastic limit of the material is approached.

† The use of an elastic hysteresis loss factor in rolling is similar in principle to the use of a coefficient of restitution e in impact problems (see §11.5). The fractional energy loss in impact is given by $1 - e^2$.

https://doi.org/10.1017/CBO9781139171731.010 Published online by Cambridge University Press

Second, the hysteresis loss factor in rolling cannot be identified with the loss factor in a simple tension or compression cycle. The deformation cycle in rolling contact, illustrated in Fig. 9.1, involves rotation of the principal axes of strain between points B, C and D, with very little change in total strain energy. The hysteresis loss in such circumstances cannot be predicted from uniaxial stress data although a plausible hypothesis has been investigated for rubber by Greenwood *et al.* (1961) with reasonable success.

A rigid sphere rolling on an inelastic deformable plane surface would produce the same deformation cycle in the surface as a *frictionless* sphere *sliding* along the surface. In spite of the absence of interfacial friction the sliding sphere would be opposed by a resistance to motion due to hysteresis in the deformable body. This resistance has been termed the 'deformation component' of friction. Its value is the same as the rolling resistance F_R given by equation (9.3). Experiments by Greenwood & Tabor (1958) with a steel ball rolling and sliding on a well-lubricated rubber surface confirm this view. They suggest that the tread of motor tyres should be made from high hysteresis rubber to introduce a large deformation resistance when skidding on the rough surface of a road in wet and slippery conditions.

To formulate a more sophisticated theory of inelastic rolling contact it is necessary to define the inelastic stress–strain relations of the solids more precisely.

9.2 Elastic-plastic materials: shakedown

In this section we shall consider the behaviour in rolling contact of solids which are perfectly elastic up to a yield point: Y in simple tension or compression, k in simple shear. Beyond yield they deform in a perfectly plastic manner according to the stress–strain relations of Reuss.

(a) Onset of yield

In free rolling, within the elastic limit, the stresses in rolling contact are given by the Hertz theory, provided the two bodies are elastically similar. The effect of dissimilar elastic properties upon the elastic-plastic behaviour, however, is generally small and will be neglected. The onset of yield in free rolling is therefore the same as in frictionless normal contact discussed in §6.1. Yield first occurs at a point beneath the surface when the maximum contact pressure $p_0 = cY$, where c is a constant (≈ 1.6) whose exact value depends upon the geometry of the contact and the yield condition used according to equations (6.4), (6.5), (6.6), (6.8) or (6.9).

In tractive rolling the shear traction at the interface influences the point of first yield. The case of complete sliding, where $Q = \mu P$, has been examined in

https://doi.org/10.1017/CBO9781139171731.010 Published online by Cambridge University Press

§7.1 (see Figs. 7.3 & 7.4). With increasing friction the point of first yield approaches the surface. In tractive rolling when $Q < \mu P$, slip only takes place over the rear part of the contact area. The stress components $\bar{\sigma}_x$ and $\bar{\tau}_{xy}$ at the surface of rolling cylinders due to the tangential traction $q(x)$ have been found in §8.3 and are shown in Fig. 9.2. Varying the value of μ whilst keeping the traction coefficient Q/P constant causes the micro-slip zone to change in size and the distribution of traction to change as shown in Fig. 9.2(*a*). When the point of first yield lies beneath the surface it is not much influenced by changes in distribution of surface traction. When first yield occurs at the surface the critical point lies at the boundary between the stick and slip zones shown in Fig. 9.2(*b*). With increasing friction the contact pressure to reach first yield falls, as shown by the broken line in Fig. 9.4.

Fig. 9.2. Stresses at contact of cylinders rolling with tangential traction $Q_x = 0.2P$. (*a*) Tangential surface tractions for varying μ; (*b*) Surface stresses σ_x and τ_{zx} for $\mu = 0.3$.

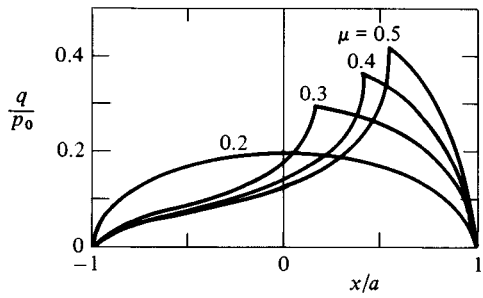

(*a*)

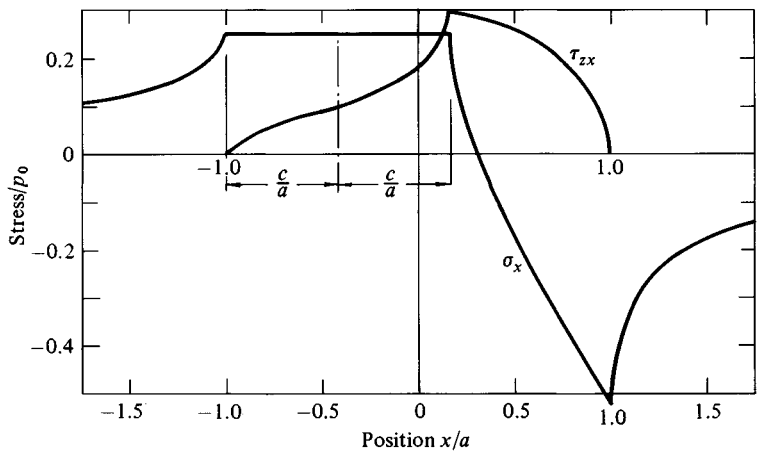

(*b*)

https://doi.org/10.1017/CBO9781139171731.010 Published online by Cambridge University Press

(b) Repeated rolling - shakedown

Most practical applications of rolling contact such as roller bearings or railway track have to withstand many repeated passes of the load. If, in the first pass, the elastic limit is exceeded some plastic deformation will take place and thereby introduce residual stresses. In the second passage of the load the material is subjected to the combined action of the contact stresses and the residual stresses introduced in the previous pass. Generally speaking such residual stresses are protective in the sense that they make yielding less likely on the second pass. It is possible that after a few passes the residual stresses build up to such values that subsequent passes of the load result in entirely elastic deformation. This is the process of *shakedown* under repeated loading, whereby initial plastic deformation introduces residual stresses which make the steady cyclic state purely elastic. To investigate whether shakedown occurs we can appeal to Melan's theorem (see Symonds, 1951) which states: if *any* time-independent distribution of residual stresses can be found which, together with the elastic stresses due to the load, constitutes a system of stresses within the elastic limit, then the system will shakedown. Conversely, if no such distribution of residual stresses can be found, then the system will not shakedown and plastic deformation will occur at every passage of the load.

We shall examine the case of an elastic cylinder rolling freely on an elastic-perfectly-plastic half-space (see Johnson, 1962*b*). If the elastic limit is not exceeded the contact area and the contact pressure are given by the Hertz theory. The stresses within the half-space are given by equations (4.49) and are shown by the full lines in Fig. 9.3 for a constant depth $z = 0.5a$. We now consider possible distributions of residual stress (denoted by suffix r) which can remain in the half-space after the load has passed. The assumption of plane deformation eliminates $(\tau_{xy})_r$ and $(\tau_{yz})_r$, and makes the remaining components independent of y. If the plastic deformation is assumed to be steady and continuous the surface of the half-space will remain flat and the residual stresses must be independent of x. Finally, for the residual stresses to be in equilibrium with a traction free surface $(\sigma_z)_r$ and $(\tau_{zx})_r$ cannot exist. The only possible system of residual stresses, therefore, reduces to

$$\left.\begin{aligned}&(\sigma_x)_r = f_1(z), \quad (\sigma_y)_r = f_2(z)\\ &(\sigma_z)_r = (\tau_{xy})_r = (\tau_{yz})_r = (\tau_{zx})_r = 0\end{aligned}\right\} \tag{9.4}$$

The principal stresses due to the combination of contact and residual stresses are given by

$$\sigma_1 = \tfrac{1}{2}\{\sigma_x + (\sigma_x)_r + \sigma_z\} + \tfrac{1}{2}[\{\sigma_x + (\sigma_x)_r - \sigma_z\}^2 + 4\tau_{zx}^2]^{1/2} \tag{9.5a}$$

$$\sigma_2 = \tfrac{1}{2}\{\sigma_x + (\sigma_x)_r + \sigma_z\} - \tfrac{1}{2}[\{\sigma_x + (\sigma_x)_r - \sigma_z\}^2 + 4\tau_{zx}^2]^{1/2} \tag{9.5b}$$

$$\sigma_3 = \nu\{\sigma_x + \sigma_z\} + (\sigma_y)_r \tag{9.5c}$$

https://doi.org/10.1017/CBO9781139171731.010 Published online by Cambridge University Press

Following Melan's theorem, we can choose the residual stresses to have any value at any depth in order to avoid yield. Thus $(\sigma_y)_r$ can be chosen to make σ_3 the intermediate principal stress. Then to avoid yield, by the Tresca criterion,

$$\tfrac{1}{4}(\sigma_1 - \sigma_2)^2 \leqslant k^2$$

where k is the yield stress in simple shear, i.e.

$$\tfrac{1}{4}\{\sigma_x + (\sigma_x)_r - \sigma_z\}^2 + \tau_{zx}^2 \leqslant k^2 \tag{9.6}$$

Examining this expression shows that it cannot be satisfied if τ_{zx} exceeds k, but it can just be satisfied with $\tau_{zx} = k$ if we choose $(\sigma_x)_r = \sigma_z - \sigma_x$. Thus the limiting condition for shakedown occurs when the maximum value of τ_{zx} anywhere in the solid just reaches k.

From equation (4.49) the maximum value of τ_{zx} is found to be $0.25p_0$ at points $(\pm 0.87a, 0.50a)$. Thus for shakedown to occur

$$p_0 \leqslant 4.00k \tag{9.7}$$

The same result is found if the von Mises criterion of yield is used. The residual stresses at a depth $0.50a$ necessary to ensure shakedown are

$$(\sigma_x)_r = -0.134p_0; \quad (\sigma_y)_r = -0.213p_0 \tag{9.8}$$

By von Mises criterion the value of p_0 for first yield is $3.1k$. Thus the ratio of the

Fig. 9.3. Rolling contact of elastic-plastic cylinders. Solid line – elastic stresses at depth $z = 0.5a$. Broken line – with addition of $(\sigma_x)_r$ and $(\sigma_y)_r$ for shakedown.

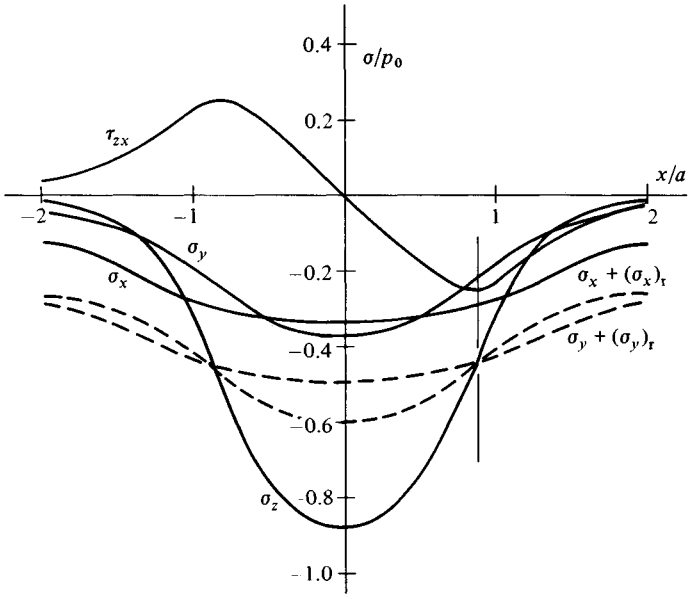

https://doi.org/10.1017/CBO9781139171731.010 Published online by Cambridge University Press

shakedown limit load to the elastic limit load is given by

$$\frac{P_S}{P_Y} = \frac{(p_0)_S^2}{(p_0)_Y^2} = 1.66 \tag{9.9}$$

from which it follows that the load must be increased by more than 66% above the first yield load to produce continuous deformation with repeated loading cycles. The modification to the stresses at $z = 0.5a$ by the introduction of the residual stresses is shown by the broken lines in Fig. 9.3.

A similar analysis can be made for tractive rolling if the elastic contact stress field is known (Johnson & Jefferis, 1963). Under conditions of complete slip or sliding the stresses in the half-space due to the frictional traction are given by equations (7.5)–(7.8). The residual stresses are still given by (9.4) and hence the shakedown limit is still determined by the maximum value of τ_{zx}. The point of maximum τ_{zx} lies below the surface provided $Q/P \leqslant 0.367$. At larger values of traction the critical stress lies in the surface layer. The influence of tangential traction on the shakedown limit is compared with its influence on initial yield in Fig. 7.4. The interval between the load for first yield and the shakedown limit load becomes narrower with increasing tangential force. The effect of partial slip on initial yield and shakedown is shown in Fig. 9.4. Shakedown of a wheel rolling on a rigid plane has been studied by Garg *et al.* (1974).

Fig. 9.4. Cylinders rolling with tangential traction $Q_x = 0.2P$. Broken line – first yield; solid line – shakedown. (Tresca yield criterion.)

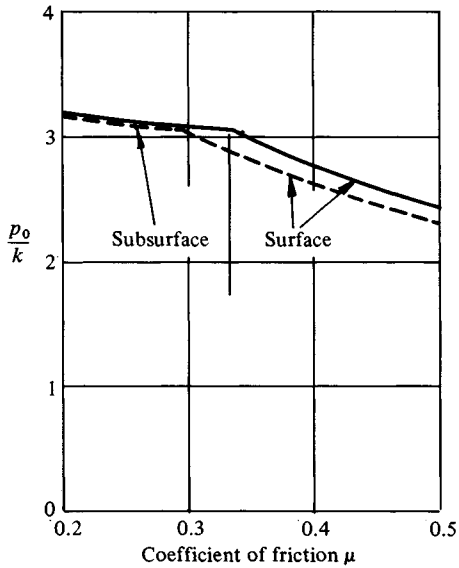

https://doi.org/10.1017/CBO9781139171731.010 Published online by Cambridge University Press

The application of Melan's Theorem to three-dimensional rolling bodies is much more complicated since all components of residual stress can arise, and since a flat surface does not remain flat after deformation. If we consider the plane of symmetry ($y = 0$) of a ball rolling on an elastic-plastic half-space, by symmetry $(\tau_{xy})_r = (\tau_{yz})_r = 0$, but a residual shear stress $(\tau_{zx})_r$ can exist. However τ_{zx} due to a purely normal contact load has equal and opposite maxima on either side of $x = 0$. Thus yield cannot be inhibited by the addition of a unidirectional residual stress. It follows, therefore, that the shakedown limit is again governed by the maximum value of $(\tau_{zx})_r$.† If the reduction in contact pressure due to the formation of a shallow plastic groove is neglected then $(\tau_{zx})_{max} = 0.21p_0$, whereupon for shakedown

$$p_0 \leqslant 4.7k \tag{9.10}$$

By von Mises, the value of p_0 for first yield is $2.8k$, hence

$$\frac{P_S}{P_Y} = \left(\frac{4.7}{2.8}\right)^3 = 4.7 \tag{9.11}$$

which is a much larger factor than in the two-dimensional case.

The mechanism of shakedown may be appreciated qualitatively from Fig. 9.1. First yield occurs in the element at C on the centre-line by shear on planes at 45° to the axes: the element is compressed normal to the surface and attempts to expand parallel to it. Since all elements at that depth are plastically deformed in this way in turn, their lateral expansion must be annulled by the development of residual compressive stresses acting parallel to the surface. When these residual stresses are fully developed the elements no longer yield at C and normal compression of the surface ceases. The alternating 'orthogonal shear' τ_{zx} of the elements at B and D on the other hand cannot be reduced by the introduction of residual shear stress $(\tau_{zx})_r$. Hence it is the 'orthogonal shear' at B and D which governs the shakedown limit and the repeated plastic deformation which occurs when the shakedown limit is exceeded.

Two additional effects contribute to apparent shakedown of surfaces in rolling contact. The first, mentioned above, is the development of a groove with three-dimensional bodies which increases the contact area and reduces the contact pressure. Thus the true shakedown limit for a circular contact is somewhat greater than that given by (9.10). This process has been studied by Eldridge & Tabor (1955) for high loads when a deep groove is formed. With repeated rolling the depth and width of the groove reached steady values, from which it was concluded that subsequent deformation was entirely elastic. The stabili-

† It can be shown that a self-equilibrating system of residual stresses can be found such that all points in the half-space do not exceed the elastic limit.

https://doi.org/10.1017/CBO9781139171731.010 Published online by Cambridge University Press

sation of the groove dimensions does not guarantee a true shakedown state, however, since plastic shear parallel to the surface (orthogonal shear) may still be taking place.

The second effect which leads to apparent shakedown is a strain hardening. With repeated deformation the value of k may rise, such that a load which initially exceeds the shakedown limit subsequently lies within it. The theory is derived for ideally plastic solids and some difficulty arises in applying it to materials which strain-harden. Ponter (1976) has extended the theory to cover an idealised material which yields initially at $k = k'$, but is capable of 'kinematic hardening' up to an 'ultimate' value of $k = k''$ ($k'' > k'$).† For shakedown Melan's theorem must be satisfied with $k = k''$. At the same time yield must be avoided, with $k = k'$, by the loading stresses in combination with apparent residual stresses *which need not satisfy the equations of equilibrium.* In the two-dimensional case discussed above, the only possible system of residual stresses, given by equation (9.4), automatically satisfies equilibrium, so that the shakedown limit for a kinematically hardening material is still given by equation (9.7) with $k = k'$. Shakedown of a three-dimensional contact has been studied for a kinematically hardening material by Rydholm (1981) and for a perfectly plastic material by Ponter *et al.* (1985).

(c) Repeated rolling - cumulative deformation

When the load exceeds the shakedown limit, from the previous discussion we should expect orthogonal plastic shear to occur in the subsurface elements B and D (Fig. 9.1). The *elastic* stresses and strains at B and D are equal and opposite, but experiments by Crook (1957) and Hamilton (1963) have shown that in free rolling a net increment of permanent shear takes place in the sense of the outflowing element at D. In repeated rolling cycles the plastic deformation accumulates so that the surface layers are displaced 'forward', i.e. in the direction of flow, relative to the deeper layers (see Fig. 9.11(a)).

An approximate analysis of the elastic-plastic behaviour has been made (Merwin & Johnson, 1963) by using the Reuss stress-strain relations in conjunction with the *elastic distribution of strain.* In this way the stress components in an element at any depth may be computed as it flows through the strained region. By this technique the condition of compatibility of strains and the stress-strain relations are satisfied exactly but the equilibrium of stresses is only satisfied approximately. However, equilibrium of the residual stresses, expressed by equations (9.4), is maintained. The assumption that the strain field, including

† This idealisation of material behaviour implies that the initial yield locus of 'radius' k' is free to translate in stress space provided that it remains inscribed within a fixed yield locus of 'radius' k''.

https://doi.org/10.1017/CBO9781139171731.010 Published online by Cambridge University Press

plastic deformation, is the same as that without it, is likely to be a reasonable one while the plastic zone is fully contained beneath the surface and therefore is constrained by the surrounding elastic material. This will be the case provided that the load is not greatly in excess of the shakedown limit.

Starting with a stress-free body a number of cycles of load must be followed. The residual stresses build up very quickly and a steady state is virtually reached after four or five cycles.

The complete numerical analysis follows the variation in all the components of stress at each depth. However, the important components of stress and strain are τ_{zx} and γ_{zx}, and the mechanism of cumulative plastic deformation can be appreciated from a simple model which considers these components only. The steady-state stress–strain cycle is illustrated in Fig. 9.5. An element approach-

Fig. 9.5. Cumulative plastic shear in rolling contact: simplified orthogonal shear stress–strain cycle experienced by an element at depth $z = 0.5a$.

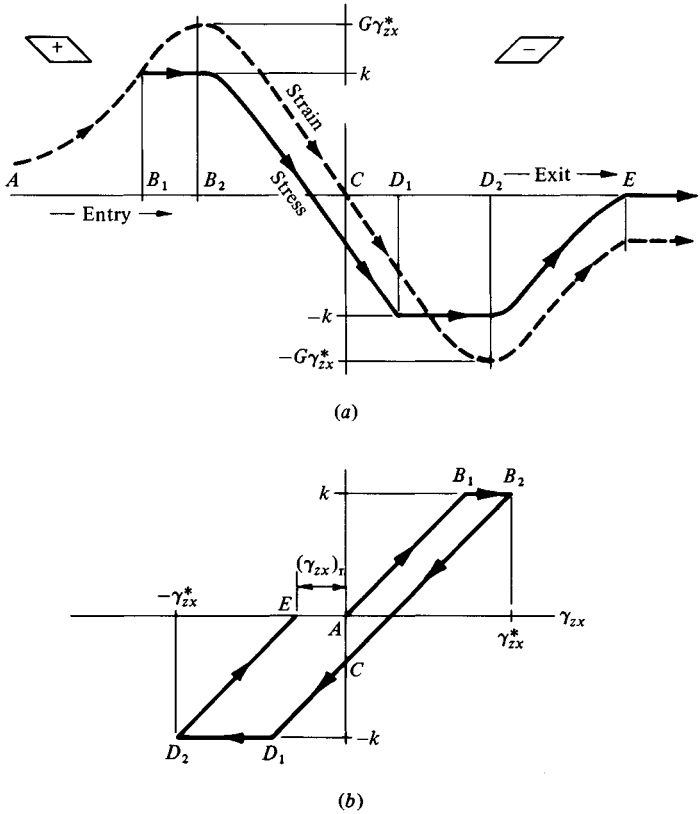

https://doi.org/10.1017/CBO9781139171731.010 Published online by Cambridge University Press

ing the loaded region deforms elastically from A to B_1 at which point the yield stress is reached ($\tau_{zx} = +k$). The element then deforms plastically at constant stress while the strain continues to increase to a maximum $\gamma_{zx} = \gamma^*_{zx}$ at B_2. From B_2, through C to D_1, the element unloads elastically and is deformed in the opposite (−ve) sense until the yield point ($\tau_{zx} = -k$) is reached at D_1. Reversed plastic deformation now takes place until the maximum negative strain, $\gamma_{zx} = -\gamma^*_{zx}$, is reached at D_2. The element then unloads until it is stress-free at E. It is not strain-free, however, since it has acquired an increment of negative residual strain $(\gamma_{zx})_r$. The forward displacement of the surface in one loading cycle is obtained by integrating $(\gamma_{zx})_r$ through the depth of the plastically deformed layer. Such calculations using the complete numerical analysis are compared with experimental measurements in Fig. 9.6.

The resistance to rolling can be calculated from computation of the total plastic work per unit distance rolled as elements flow through the plastic zone. On the first pass the plastic zone extends through a depth corresponding to that in which the elastic stresses, could they be realised, would exceed the plastic limit. In the steady state, continuous plastic deformation is restricted to a narrower layer (see Fig. 9.7). The resistance to rolling is then much less than

Fig. 9.6. Cumulative plastic shear in rolling contact: Merwin & Johnson theory (1963) compared with experiments: circle – Cu/Cu; triangle – Cu/Al; square – Cu/steel.

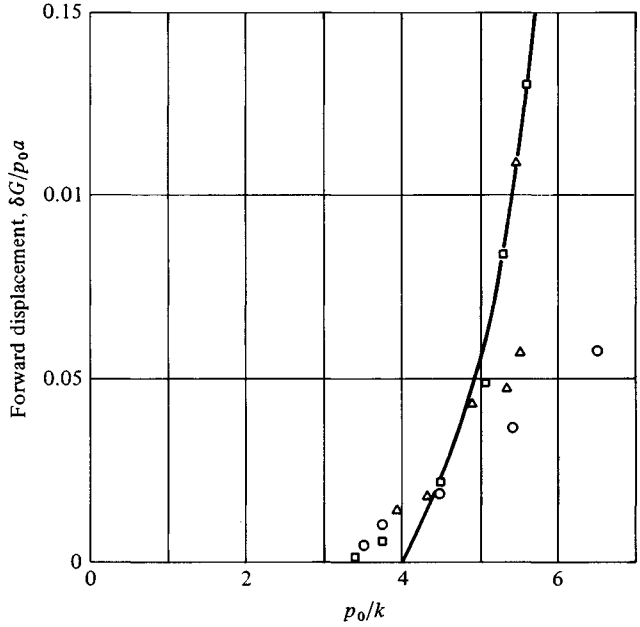

https://doi.org/10.1017/CBO9781139171731.010 Published online by Cambridge University Press

Fig. 9.7. Residual stresses induced in free rolling contact of Duralumin rollers. Circumferential stress $(\sigma_x)_r$: solid line – calculated; plus signs joined by dashes – measured. Axial stress $(\sigma_y)_r$: broken line – calculated; chain line – measured.

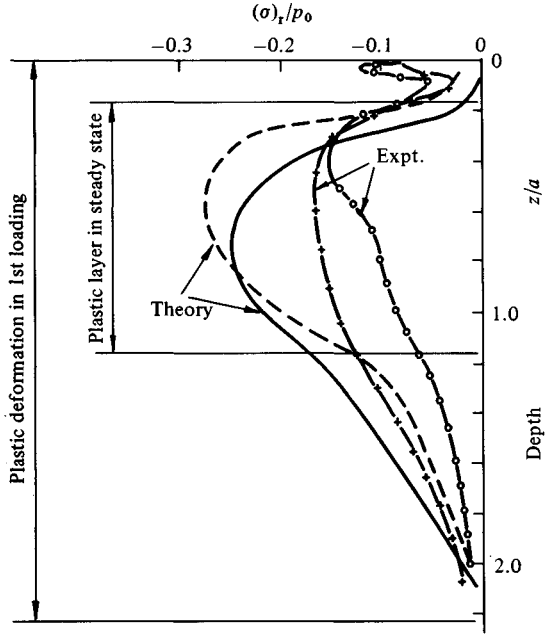

in the first pass, although it is still much larger than would normally be expected from elastic hysteresis (see Fig. 9.13).

Finally the analysis predicts the residual stresses $(\sigma_x)_r$ and $(\sigma_y)_r$ which are introduced by plastic deformation. The calculated variation with depth for $p_0 = 4.8k$ is shown in Fig. 9.7. Measurements by Pomeroy & Johnson (1969) of the circumferential and axial components of residual stress in an aluminium alloy disc due to free rolling contact are also plotted in Fig. 9.7. In their main features the agreement between theory and experiment is satisfactory; both components of stress are compressive; they arise in the layer in which the elastically calculated stresses exceed the elastic limit; the maximum values coincide roughly with the depth at which τ_{zx} is a maximum. The values of the measured stresses are appreciably lower than calculated. This discrepancy is likely to be due largely to the lack of plane-strain conditions in the experiment.

9.3 Rolling of a rigid cylinder on a perfectly plastic half-space

At high loads the plastic zone beneath a roller spreads to the free surface so that large plastic strains are possible. In these circumstances the stresses may

https://doi.org/10.1017/CBO9781139171731.010 Published online by Cambridge University Press

be analysed by neglecting the elastic strains and making use of the theory of rigid-perfectly-plastic solids. In general the roller supports a normal load P, a tangential force Q and a moment M_G applied to the centre of the roller, shown in the positive sense in Fig. 9.8. A driving wheel has M_G positive and Q negative whereas a braked wheel has M_G negative and Q positive; in free rolling $Q = 0$. The mode of plastic deformation depends upon the magnitude and sign of the applied forces.

We shall consider first the case of Q positive, and assume that friction is sufficient to prevent slip at the interface. Incompressibility of the material and plane deformation require that, in the steady state, the level of the surface is unchanged by the roller. An approximate slip-line field and hodograph proposed by Mandel (1967) for this case are shown in Fig. 9.9(a). The cap of material ODC adheres to the roller and rotates with it about an instantaneous centre I fixed to the half-space. A velocity discontinuity follows the slip line $ABCO$. It is clear from the hodograph that the velocity of the free surface at D is somewhat greater than at A so that the actual surface AD must be slightly concave and in consequence the slip lines DB and DC cannot be perfectly straight as shown. However the errors will not be large provided that the ratio of contact size to roller radius a/R is not too large.

The geometry of the field is specified by the two independent parameters: (a/R) and the angle α. The pressure on DC is then given by

$$p_{DC} = k(1 + \pi/2 + 2\alpha - 2\psi) \tag{9.12}$$

and that on OC by

$$p_{OC} = k(1 + \pi/2 + 2\theta - 2\psi) \tag{9.13}$$

By integrating the stresses along DC and CO the forces P and Q and the moment

Fig. 9.8. Rolling contact of a rigid cylinder on a rigid perfectly-plastic half-space.

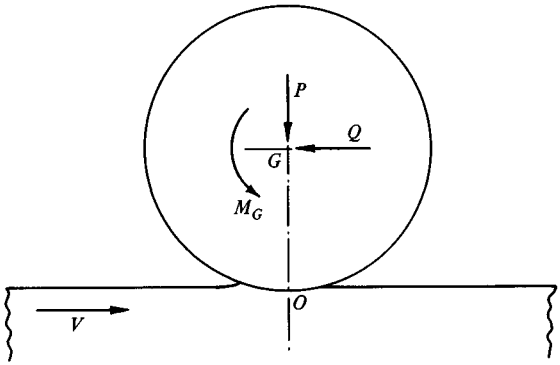

https://doi.org/10.1017/CBO9781139171731.010 Published online by Cambridge University Press

Fig. 9.9. Slip-line fields for a rigid cylinder rolling on a rigid-perfectly-plastic half-space (Mandel, 1967). (*a*) Mode I, (*b*) Mode II, Mode III.

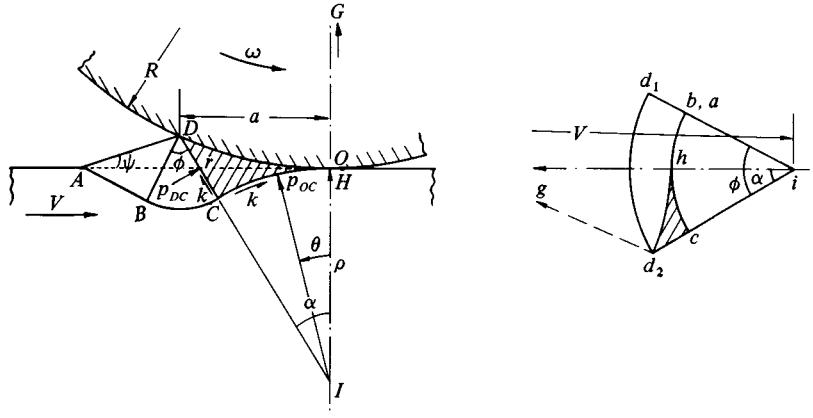

(*a*)

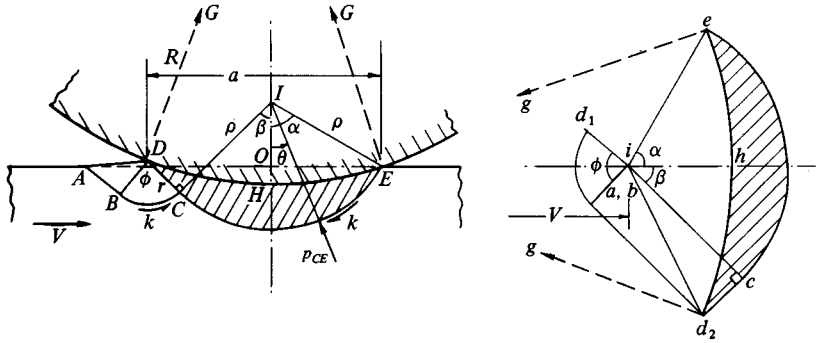

(*b*)

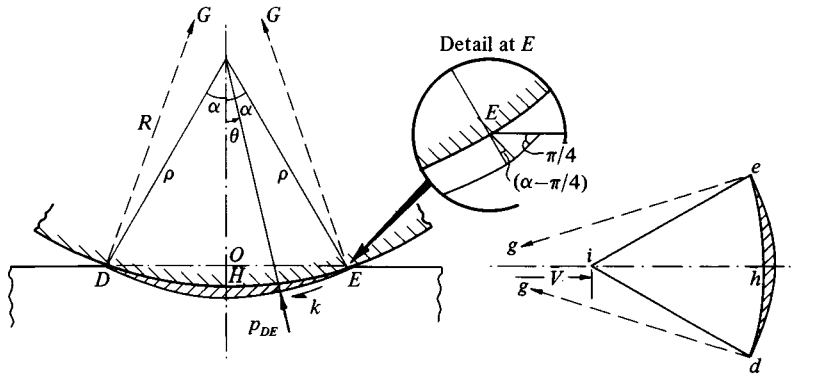

(*c*)

https://doi.org/10.1017/CBO9781139171731.010 Published online by Cambridge University Press

M_G can be found. Mandel simplifies his analysis still further for small values of a/R by assuming that the deformed surface ADO remains flat whereupon the angle $\psi = 0$. The solution is then a function of the single independent variable α only. This approximation is reasonable when I is located close to O and α is large, which is the case in the vicinity of free rolling. Under conditions of severe braking, on the other hand, the angle α becomes small and ψ is no longer small in comparison. In the limiting case of a locked wheel which slides without rotating, I moves to an infinite distance beneath the surface, $\alpha \to 0$, and $\psi \to \pi/4$. The limiting slip-line field comprises a small wedge of material which shears along the line AO. This is the same situation as that of a sliding wedge discussed in §7.6(*b*) and shown in Fig. 7.19(*b*). In this limit

$$P = Q = k(a + a^2/2R) \tag{9.14}$$

Taking moments about O

$$M_O = M_G + QR = \tfrac{1}{2}ka^2(1 + a/R + a^2/4R^2) = \tfrac{1}{2}P^2/k \tag{9.15}$$

The values of P, Q and M_O have been calculated for a range of values of α using the geometry of the field shown in Fig. 9.9(*a*) together with the equations (9.12) and (9.13). The results are plotted in non-dimensional form as $M_O k/P^2$ against the ratio Q/P and give the curve on the right-hand side of Fig. 9.10. The relationship has been computed for a value of $a/R = 0.2$, but this curve is almost independent of the value a/R, provided that a/R is not too large.

The pattern of plastic deformation is determined by the hodograph. To a first approximation surface points in the deforming region have a horizontal velocity from right to left relative to the body of the solid given by $ih - \omega\rho$. The forward velocity of the roller centre $V = \omega(R + \rho)$, so that the time of passage of a surface point through the deforming region from A to O is given by

$$T = AH/V \approx (\sqrt{(2)}\, r + a)/\omega(R + \rho)$$

where $r = DC$ and $\rho = IO$ as shown in Fig. 9.9(*a*). The plastic displacement of this surface Δ is thus given by $\Delta = -\omega\rho T$, i.e.

$$\frac{\Delta}{R} = -\frac{\rho(a + \sqrt{(2)}\, r)}{R(R + \rho)} \tag{9.16}$$

The surface of the half-space is displaced permanently *backwards* by the rolling action. This is in contrast with the behaviour at lighter loads, described in the previous section, where the action of the surrounding elastic material causes the surface to be displaced *fowards.* (See Fig. 9.11).

Two special cases call for comment.

(i) The condition of free rolling is specified by $Q/P = 0$ ($\alpha = 73.5°$), whereupon

$$M_O = M_G = 0.104P^2/k \tag{9.17}$$

https://doi.org/10.1017/CBO9781139171731.010 Published online by Cambridge University Press

(ii) The situation of a wheel driven forward by a horizontal force through a frictionless bearing at G (i.e. $M_G = 0$) is specified by $M_O = QR$ and is located therefore in Fig. 9.10 by the intersection of the curve by a straight line of gradient Rk/P. The resistance to rolling in this case is slightly greater than in free rolling.

An exact analysis of the deformation in Mode I shown in Fig. 9.9(a) has been made by Collins (1978), in which the free surface AD takes in correct concave profile and the slip lines DC and DB are appropriately curved. The exact results are shown by the broken lines in Fig. 9.10. They depend upon M_G as well as upon Q, but the difference from Mandel's approximate theory is not large. It has been pointed out by Petryk (1983) that even Collins' exact solutions are not unique, but the possible range of variation is not large except at high loads when the limit of complete shear ($Q/P = 1$) is approached.

As I approaches O and the angle α increases, the material to the right of CO becomes overstressed and deforms plastically. The new mode of deformation has not been found with certainty. Mandel proposes the mode shown in Fig. 9.9(b) with a velocity discontinuity along the line DCE and a stress discontinuity at E. The cap DCE adheres to the roller and rotates with it about an instantaneous centre I which now lies above O. The pressure along CE is given by:

$$p_{CE} = k\{1 + 2\alpha - 2\theta - \sin(\alpha - \pi/4)\} \tag{9.18}$$

and the angle β is determined by equating the values of the pressure at C given

Fig. 9.10. Rolling moments and forces given by the slip-line fields of Fig. 9.9.

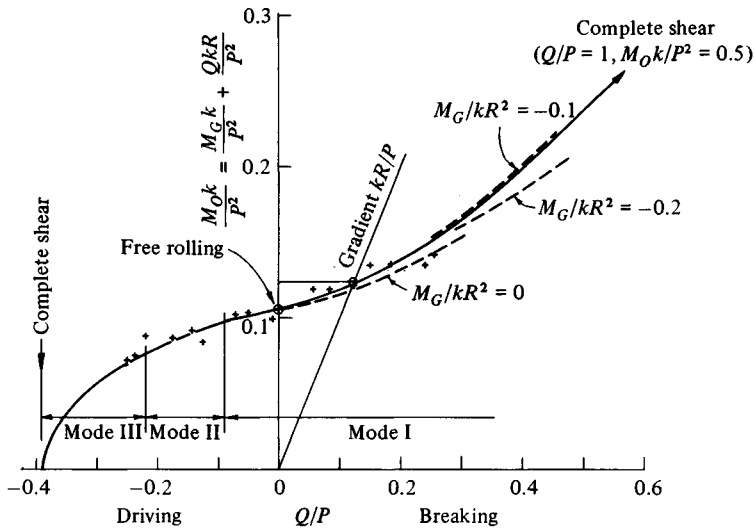

https://doi.org/10.1017/CBO9781139171731.010 Published online by Cambridge University Press

Fig. 9.11. Plastic deformation in rolling contact: (*a*) moderate loads – cumulative forward displacement (see §9.2(*c*)); (*b*) heavy loads – backward displacement in one pass (see eq. (9.16)).

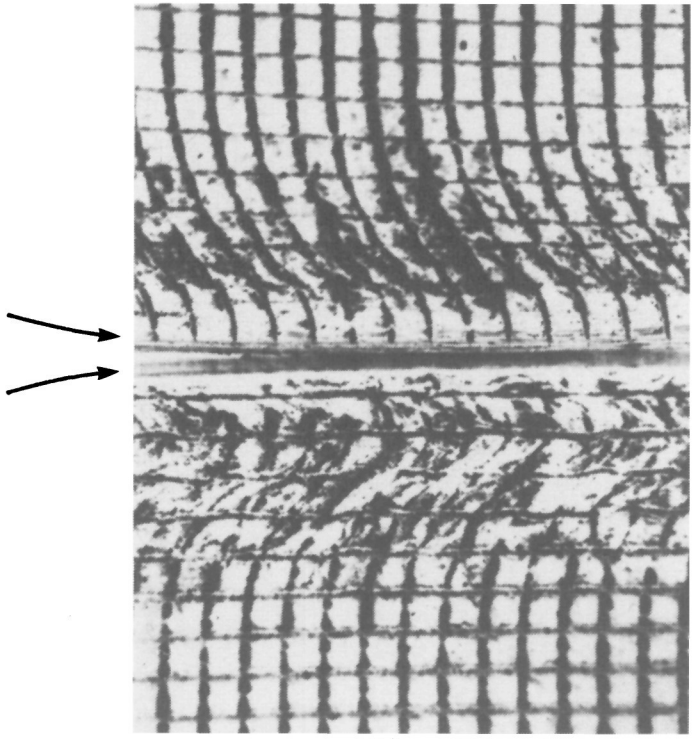

(*a*)

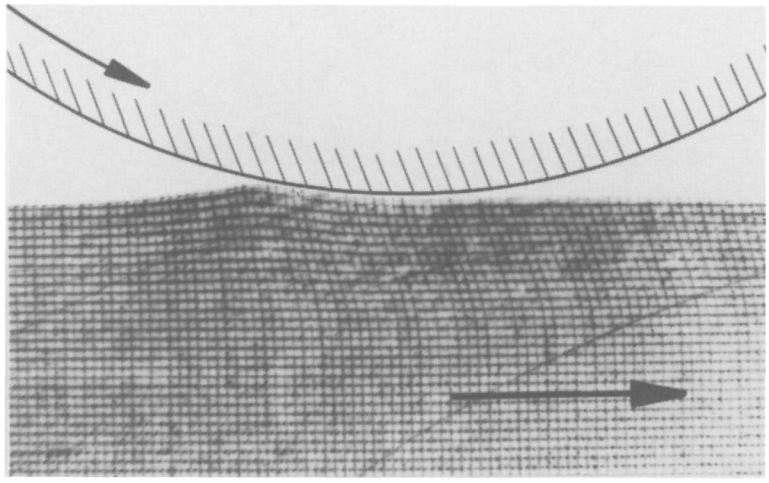

(*b*)

https://doi.org/10.1017/CBO9781139171731.010 Published online by Cambridge University Press

by equations (9.12) and (9.18). Mandel estimates that the change from the first to the second mode of deformation takes place at $Q/P = -0.09$. The change is accompanied by a large increase in contact area and a change in sign of the permanent displacement of the surface which is now given by

$$\frac{\Delta}{R} = \frac{a(\rho \cos\alpha - r^2/a)}{R(R - \rho\cos\alpha)} \tag{9.19}$$

However the moment M_O decreases in a continuous manner between the two modes as shown in Fig. 9.10.

With an increase in driving moment on the cylinder the mode of deformation changes again, when $\alpha \leqslant \pi/4$, to a single velocity discontinuity along the arc DE as shown in Fig. 9.9(*c*). A vanishingly small fan of angle $(\pi/4 - \alpha)$ is located with its apex at E, whereupon the pressure on the slip line DE is

$$p_{DE} = k(1 + \pi/2 - 2\theta) \tag{9.20}$$

Integrating the stresses along this slip line completes the variation in M_O with Q/P shown in Fig. 9.10. Complete shear, which corresponds to the spinning of a driving wheel, occurs when $\alpha \to 0$, i.e. when $Q/P \to -1/(1 + \pi/2)$.

The analysis outlined above assumes complete sticking along the arc of contact. In each mode of deformation the contact pressure is least at the trailing edge of contact, so slip would be expected to initiate there. A modification to the first mode of deformation, which includes micro-slip at the rear of the arc of contact, has been given by Mandel (1967), and also by Segal (1971). The effect is to reduce the values of M_O in Fig. 9.10 slightly and to restrict the limiting value of Q/P. A complete analysis for the case of zero interfacial friction has been presented by Marshall (1968). In this case M_G must be zero and Marshall finds that

$$M_O = QR = \frac{P^2 k}{2(2+\pi)} \left\{1 + \frac{P}{6(2+\pi)kR}\right\} \tag{9.21}$$

Taking a typical value of $P/kR = 1.0$, equation (9.21) gives $M_O/P^2k = 0.100$. Drawing a line of slope 1.0 on Fig. 9.10 gives a value of $M_O/P^2k = 0.125$, so that complete adhesion increases the resistance to rolling by 25% above the frictionless value.

Rolling resistance measurements by Mandel with a steel cylinder rolling on a lead surface are included in Fig. 9.10. The value of k for the lead has been chosen to fit the experiments to the theory at the free rolling point ($Q = 0$), but the theoretical variation in M_O with Q/P at constant load is well supported by the observations. They confirm that there is no discontinuity in M_O in changing from driving to braking. Absolute measurements of rolling resistance and surface displacements by Johnson & White (1974) with steel rolling on copper for the special cases of $Q = 0$ and $M_G = 0$ gave the results shown in

Table 9.1

P/kR		$Q = 0$		$M_G = 0$	
		M_G/RP	Δ/R	Q/P	Δ/R
0.73	Theory	0.076	−0.013	0.085	−0.030
	Experiment	0.047	−0.007	0.053	−0.012
1.05	Theory	0.110	−0.017	0.130	−0.042
	Experiment	0.078	−0.016	0.085	−0.032

Table 9.1. The general trend of the measurements follows the results of Mandel's theory but the observed magnitude of both the rolling resistance and the surface displacements is less than predicted. The discrepancies are almost certainly due to the influence of elastic deformation, and they emphasise that a rigid-perfectly-plastic analysis sets an upper limit on the rolling resistance and the amount of permanent deformation.

9.4 Rolling contact of viscoelastic bodies

When the stress in the material of a body in rolling contact is influenced by the *rate* of strain, the contact stresses and deformation will depend upon the speed of rolling. The simplest time-dependent constitutive relations for a material are those described as linear viscoelastic. They have been discussed in §6.5 in relation to normal contact. Even so, the application of the linear theory of viscoelasticity to rolling is not simple, since the situation is not one in which the viscoelastic solution can be obtained directly from the elastic solution. The reason for the difficulty is easy to appreciate. During rolling the material lying in the front half of the contact is being compressed, whilst that at the rear is being relaxed. With a perfectly elastic material the deformation is reversible so that both the contact area and the stresses are symmetrical about the centre-line. A viscoelastic material, on the other hand, relaxes more slowly than it is compressed so that the two bodies separate at a point closer to the centre-line than the point where they first make contact. Thus, in Fig. 9.12, $b < a$ and recovery of the surface continues after contact has ceased. The geometry of the rolling contact problem in viscoelasticity is different, therefore, from that in the perfectly elastic case so that the viscoelastic solution cannot be obtained directly from the elastic solution. Furthermore the point of separation ($x = b$) cannot be prescribed; it has to be located subsequently as the point where the contact pressure falls to zero.

In view of these difficulties we shall present a one-dimensional treatment in which a viscoelastic solid is modelled by a simple viscoelastic foundation of parallel compressive elements which do not interact with each other (May *et al.*, 1959). We shall consider the contact of a rigid frictionless cylinder of radius R rolling on such a foundation, as shown in Fig. 9.12.

The rolling velocity is V and the cylinder makes first contact with the solid at $x = -a$. Since there is no shear interaction between the elements of the foundation, the surface does not depress ahead of the roller. To the usual approximation, for $a \ll R$, the strain (compressive) in an element of the foundation at x is given by

$$\epsilon = -(\delta - x^2/2R)/h, \quad -a \leqslant x \leqslant b \tag{9.22}$$

where δ is the maximum depth of penetration of the roller.

If the foundation were perfectly elastic with modulus K, the contact would be symmetrical ($b = a$) and the stress in each element σ would be $K\epsilon$. The pressure distribution under the roller and the total load would then be given by equations (4.58) and (4.59). For a viscoelastic material the elastic modulus K is replaced by a relaxation function $\Psi(t)$ as explained in §6.5. Thus by equation (6.51) the stress in the viscoelastic element at x is given by

$$p(x, t) = -\sigma = -\int_0^t \Psi(t - t') \frac{\partial \epsilon(t')}{\partial t'} \, dt' \tag{9.23}$$

In steady rolling $\partial/\partial t = V\partial/\partial x$, thus, from equation (9.22) for the strain,

$$\partial\epsilon/\partial t = Vx/Rh$$

Substituting in (9.23) and changing the variable from t to x, we get

$$p(x) = -\frac{1}{Rh}\int_{-x}^{x} x'\Psi(x - x') \, dx' \tag{9.24}$$

Fig. 9.12. Rolling of a rigid cylinder on a viscoelastic foundation.

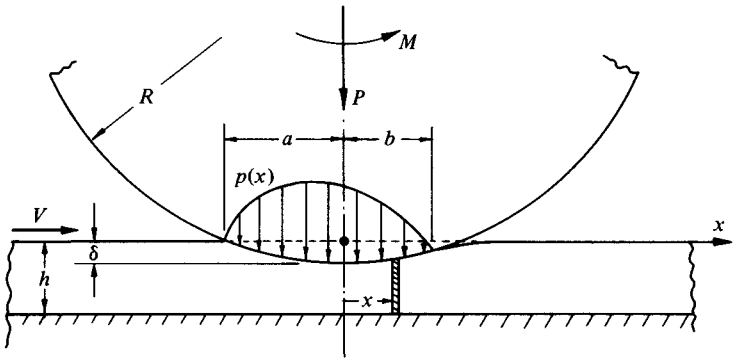

https://doi.org/10.1017/CBO9781139171731.010 Published online by Cambridge University Press

To proceed further we must specify the relaxation function for the material. Two simple examples incorporating delayed elasticity and steady creep were discussed in §6.5 (see Fig. 6.20). We shall make use of the first of these simple models, whose relaxation function is given by equation (6.54), and shall write

$$\Psi(t) = K(1 + \beta e^{-t/T}) \tag{9.25}$$

This material has an initial dynamic elastic response with modulus $K(1+\beta)$, but under static (relaxed) conditions the modulus is K and T the relaxation time. Substituting this relaxation function into equation (9.24), changing the variable from t to x and performing the integration give an expression for the pressure distribution:

$$p(x) = \frac{Ka^2}{Rh}\left[\tfrac{1}{2}(1 - x^2/a^2) - \beta\zeta(1 + x/a) + \beta\zeta(1+\zeta)\{1 - e^{-(1+x/a)/\zeta}\}\right] \tag{9.26}$$

where $\zeta = VT/a$, which represents the ratio of the relaxation time of the material to the time taken for an element to travel through the semi-contact-width a. It is sometimes referred to as the 'Deborah Number'.

The pressure is zero at $x = -a$ and falls to zero again where $x = b$; this latter condition determines the value of b/a as a function of β and ζ.

The normal load is found from

$$P = \int_{-a}^{b} p(x)\,dx = \frac{Ka^3}{Rh} F_P(\beta, \zeta) \tag{9.27}$$

and, since the pressure is now asymmetrical, rolling is resisted by a moment given by

$$M = -\int_{-a}^{b} xp(x)\,dx = \frac{Ka^4}{Rh} F_M(\beta, \zeta) \tag{9.28}$$

Thus the coefficient of rolling resistance may be expressed as:

$$\mu_R = M/PR = \frac{a}{R} F_R(\beta, \zeta) \tag{9.29}$$

Computations have been carried out for a material in which $\beta = 1.0$; values of b/a and μ_R are plotted as a function of ζ_0 ($=VT/a_0$) in Fig. 9.13, where a_0 is the static semi-contact-width. This diagram displays the significant features of visco-elastic rolling contact.

At slow rolling speeds, when the contact time is long compared with the relaxation time of the material ($\zeta_0 \ll 1$), the pressure distribution (9.26) and load (9.27) approximate to the results for a perfectly elastic material of modulus K given in equations (4.58) and (4.59). The moment M approaches zero.

https://doi.org/10.1017/CBO9781139171731.010 Published online by Cambridge University Press

At very high speeds ($\zeta_0 \gg 1$), the pressure distribution and load again approximate to the elastic results but this time with a 'dynamic' foundation modulus $K(1+\beta)$. Relaxation effects are important only when the contact time is roughly equal to the relaxation time of the material ($\zeta_0 \sim 1$). It is under these conditions that the contact becomes appreciably asymmetric and the maximum resisting moment arises. A similar analysis for a rigid sphere rolling on a viscoelastic foundation has been made by Flom & Bueche (1959).

The above analysis has been presented for a rigid cylinder rolling on a viscoelastic plane. As in elastic theory, it is equally valid to the same degree of approximation if the cylinder is viscoelastic and the plane rigid. The analysis again holds for two viscoelastic bodies if an equivalent relaxation function is used for a series combination of material elements of each body. An appropriate value for the ratio K/h of the foundation can be obtained by comparing the static deformation with Hertz as discussed in §4.3.

Fig. 9.13. Rolling of a rigid cylinder on a viscoelastic half-space ($\beta = 1$). Solid line – full solution, Hunter (1961). Large-dashed line – viscoelastic foundation model, eqs (9.26)–(9.29). Small-dashed line – loss tangent, eq. (9.36). (*a*) Contact dimensions; (*b*) rolling resistance.

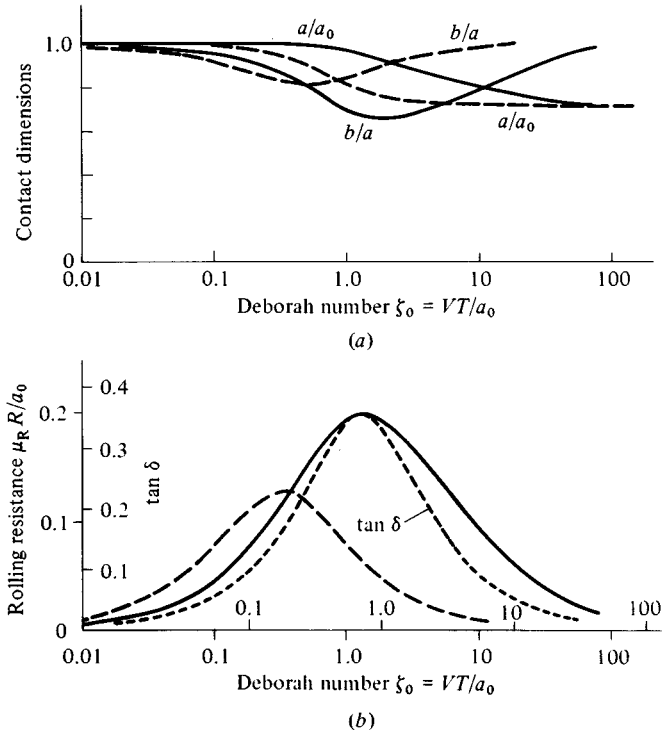

https://doi.org/10.1017/CBO9781139171731.010 Published online by Cambridge University Press

A full solution for the rolling contact of a rigid cylinder on a viscoelastic half-space has been presented by Hunter (1961) for materials having a single relaxation time. A different method, which is capable of handling two viscoelastic bodies having general relaxation functions, has been developed by Morland (1967*a* & *b*) but considerable computing effort is necessary to obtain numerical results.

For a rigid cylinder rolling on a simple material whose relaxation function is given by (9.25) Hunter's and Morland's solutions are identical. Results for a material whose Poisson's ratio ν is constant and $\beta = 1$ are plotted in Fig. 9.13, where they are compared with the one-dimensional foundation model. The qualitative behaviour of the simple model is similar to that given by the full analysis; the contact is most asymmetrical and the rolling resistance is a maximum at a Deborah Number of about unity. The rolling moment peak is lower for the model since energy dissipated in shear between the elements is ignored and the peak occurs at a somewhat lower value of VT/a_0 since the length of the deforming zone in the model is less than that in the half-space.

Materials having more than one relaxation time would exhibit a rolling resistance peak whenever the time of passage through the contact coincided with one of the relaxation times.

9.5 Rolling friction

Ideally rolling contact should offer no resistance to motion, but in reality energy is dissipated in various ways which give rise to 'rolling friction'. Much of the analysis discussed in this chapter and the previous one has been the outcome of attempts to elucidate the precise mechanism of rolling resistance, so that it would seem appropriate to conclude this chapter with a summary of our present understanding. The various sources of energy dissipation in rolling may be classified into (*a*) those which arise through micro-slip and friction at the contact interface, (*b*) those which are due to inelastic properties of the material and (*c*) those due to roughness of the rolling surfaces. We shall consider each in turn.

'Free rolling' has been defined as motion in the absence of a resultant tangential force. Resistance to rolling is then manifest by a couple M_y which is demanded by asymmetry of the pressure distribution: higher pressures on the front half of the contact than the rear. The trailing wheels of a vehicle, however, rotate in bearings assumed frictionless and rolling resistance is overcome by a tangential force Q_x applied at the bearing and resisted at the contact interface. Provided that the rolling resistance is small ($Q_x \ll P$) these two situations are the same within the usual approximations of small strain contact stress theory, i.e. to first order in (a/R). It is then convenient to write the rolling resistance as

https://doi.org/10.1017/CBO9781139171731.010 Published online by Cambridge University Press

a non-dimensional coefficient μ_R expressed in terms of the rate of energy dissipation $\dot{W}$, thus

$$\mu_R \equiv \frac{M_y}{PR} = \frac{Q_x}{P} = \frac{\dot{W}}{PV} \tag{9.30}$$

The quantity $\dot{W}/V$ is the energy dissipated per unit distance rolled.

(a) Micro-slip at the interface

Micro-slip has been shown to occur at the interface when the rolling bodies have dissimilar elastic constants (§8.2). The resistance from this cause depends upon the difference of the elastic constants expressed by the parameter β (defined by eq. (5.3)) and the coefficient of slipping friction μ. The resistance to rolling reaches a maximum value of

$$\mu_R = \frac{M_y}{PR} \approx 15 \times 10^{-4} \beta (a/R) \tag{9.31}$$

when $\beta/\mu \approx 5$. Since, for typical combinations of materials, β rarely exceeds 0.2, the rolling resistance from this cause is extremely small.

It has frequently been suggested that micro-slip will also arise if the *curvatures* of two bodies are different. It is easy to see that the difference in strain between two such surfaces will be second-order in (a/R) and hence negligible in any small strain analysis. A special case arises, however, when a ball rolls in a closely conforming groove. The maximum rolling resistance is given by (see §8.5)

$$\mu_R = \frac{M_y}{PR} = 0.08\mu(a/R)^2(b/a)^2 \tag{9.32}$$

The shape of the contact ellipse (b/a) is a function of the conformity of the ball and the groove; where the conformity is close, as in a deep groove ball-bearing, $b \gg a$ and the rolling resistance from this cause becomes significant.

In tractive rolling, when large forces and moments are transmitted between the bodies, it is not meaningful to express rolling resistance as Q_x or M_y/R. Nevertheless energy is still dissipated in micro-slip and, for comparison with free rolling, it is useful to define the effective rolling resistance coefficient $\mu_R = \dot{W}/VP$. This gives a measure of the loss of efficiency of a tractive drive such as a belt, driving wheel or variable speed gear. In the case of the belt drive (§8.1) for example, a moment M is transmitted between the two shafts but the driven shaft runs slightly slower than the driver, the difference between input and output power being accounted for by the energy dissipated in micro-slip given by

$$\dot{W}/V = M\left(\frac{V_1}{R_1} - \frac{V_2}{R_2}\right)/V = M\xi/R \tag{9.33}$$

https://doi.org/10.1017/CBO9781139171731.010 Published online by Cambridge University Press

where ξ is the creep ratio. This approach applies also to the tractive rolling of other elastic bodies. For rolling cylinders transmitting a tangential force Q_x the creep is given by equation (8.26) whence

$$\mu_R \equiv \dot{W}/VP = \frac{\mu Q_x}{P}\{1-(1-Q_x/\mu P)^{1/2}\}\frac{a}{R}$$

$$\begin{cases} \approx \frac{1}{2}(Q_x/P)^2(a/R) & \text{for} \quad (Q_x/P) \ll \mu \qquad (9.34a) \\ = \mu^2(a/R) & \text{for} \quad (Q_x/P) = \mu) \qquad (9.34b) \end{cases}$$

on the point of gross sliding. Similar expressions for the effective rolling resistance of spherical bodies transmitting tangential forces Q_x or Q_y can be obtained from the creep equations (8.45) and (8.46). If the tractive force is small compared with the limiting friction force it is clear from (9.34*a*) that the energy loss is small, but as sliding is approached the loss may become important if the coefficient of friction is high.

Finally micro-slip is introduced by spin. The angular velocity of spin ω_z is resisted by a spin moment M_z, given by equation (8.43) provided ω_z is small. At large spins the moment rises to a maximum value $3\pi\mu Pa/16$ for a circular contact area, whereupon

$$(\mu_R)_{max} = M_z\omega_z/VP = \frac{3\pi\mu}{16}\left(\frac{\omega_z R}{V}\right)\frac{a}{R} \qquad (9.35)$$

which accounts for a serious loss of efficiency of rolling contact variable speed drives.

(b) Inelastic deformation of the material

Except in the special cases mentioned above resistance to free rolling is dominated by inelastic deformation of one or both bodies. In this case the energy is dissipated within the solids, at a depth corresponding to the maximum shear component of the contact stresses, rather than at the interface. With materials having poor thermal conductivity the release of energy beneath the surface can lead to high internal temperatures and failure by thermal stress (Wannop & Archard, 1973).

The behaviour of metals is generally different from that of non-metals. The inelastic properties of metals (and hard crystalline non-metallic solids) are governed by the movement of dislocations which, at normal temperatures, is not appreciably influenced either by temperature or by rate of deformation. Lower density solids such as rubber or polymers tend to deform in a visco-elastic manner which is very sensitive to temperature and rate of deformation.

The rolling friction characteristics of a material which has an elastic range of stress followed by rate-independent plastic flow above a sharply defined yield

https://doi.org/10.1017/CBO9781139171731.010 Published online by Cambridge University Press

stress, typical of hard metals, are shown in Fig. 9.14. Non-dimensional rolling resistance ($G\mu_R/k$) is plotted against non-dimensional load (GP/k^2R) for the contact of a rigid cylinder on a deformable solid, where G is the shear modulus and k the yield stress in shear of the solid. At low loads the deformation is predominantly elastic and the rolling resistance is given by the elastic hysteresis equation (9.2). The hysteresis loss factor α, found by experiment, is generally of the order of a few per cent.

The elastic limit is reached in the first traversal at a load given by equations (6.5) and (6.7) but, after repeated traversals, continuous plastic deformation takes place only if the load exceeds the shakedown limit given by equation (9.9). The resistance due to contained plastic deformation has been calculated by Merwin & Johnson (1963) for loads which do not greatly exceed the shakedown limit. At high loads, when the plastic zone is no longer contained, i.e. the condition of full plasticity is reached, the rolling resistance may be estimated by the rigid-plastic theory of Mandel. The onset of full plasticity cannot be precisely defined but, from our knowledge of the static indentation behaviour where full plasticity is reached when $P/2a \approx 2.6$ and $Ea/YR \approx 100$, it follows that $GP/k^2R \approx 300$. Extrapolating the elastic-plastic results completes the picture.

Fig. 9.14. Rolling resistance of a rigid cylinder on an elastic-plastic solid.

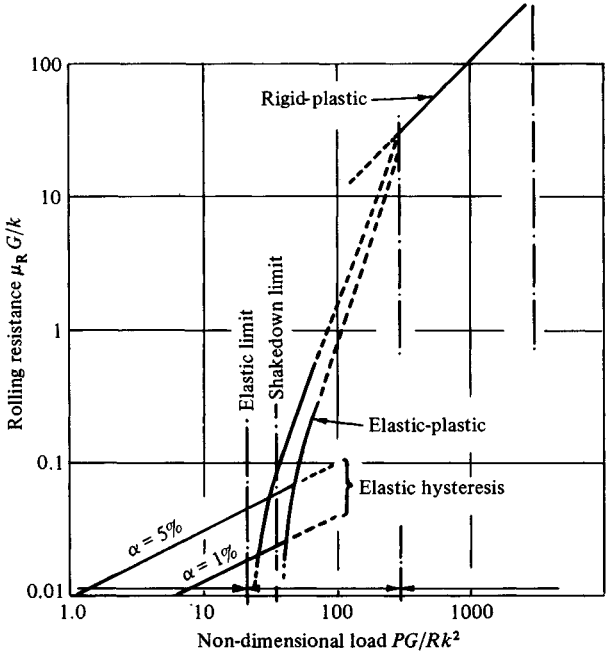

https://doi.org/10.1017/CBO9781139171731.010 Published online by Cambridge University Press

Experiments by Hamilton (1963) suggest that the elastic-plastic theory, which neglects losses in the elastically deformed material, under-estimates the rolling resistance, whilst experiments by Johnson & White (1974) suggest that the rigid-plastic theory, which neglects elastic deformation, overestimates the resistance. Nevertheless the general agreement is satisfactory and the figure shows that a steep rise in rolling resistance is to be expected when a continuously deforming plastic zone develops beneath the surface.

The characteristics of viscoelastic materials are somewhat different. In the previous section we saw how the rolling resistance of a simple linear viscoelastic solid could be analysed. Unfortunately most real viscoelastic materials are nonlinear and, further, their relaxation behaviour cannot usually be expressed in terms of a single relaxation time such as in the models shown in Fig. 6.20. However a useful empirical approach is possible using expressions (9.2) and (9.3) for rolling resistance in terms of an elastic hysteresis factor α. The most common method of measuring the hysteresis properties of viscoelastic materials is to measure the dissipation in cyclic strain as a function of frequency. The results of such measurements are usually expressed as a loss tangent $\tan\delta$, where δ is the phase angle between stress and strain. To correlate values of $\tan\delta$ with rolling resistance we compare the hysteresis theory with the full analysis given in §4 for the simple material whose relaxation function is given by (9.25). For such a material the loss tangent is given by

$$\tan\delta(\omega) = \beta\omega T/\{1 + (1+\beta)\omega^2 T^2\} \tag{9.36}$$

where T is the relaxation time of the material. This relationship for $\beta = 1$ is compared with the variation of rolling resistance with Deborah Number ζ_0 ($= VT/a_0$) in Fig. 9.13(b). The curves are similar in shape. Their peaks can be made to coincide if ωT is put equal to 1.83ζ, i.e. the period of cyclic strain is put approximately equal to the time of passage of a material element through the contact zone. Their peak values agree if the value of α in equation (9.2) is taken to be about $2.6\tan\delta$. In this way the rolling resistance for viscoelastic materials may be estimated from measurements of the loss tangent in cyclic strain, provided that the shear stress level at which the measurements are made is roughly comparable with that in rolling contact.

The variation of hysteresis loss with temperature in viscoelastic materials has been found to be related to the variation with frequency such that a unique curve is obtained when $\tan\delta$ is plotted against $a_T\omega$, where a_T is the Williams, Landen & Ferry shift factor defined by (see Ward, 1971)

$$\ln a_T = \frac{C_1(\theta - \theta_s)}{C_2 + (\theta - \theta_s)} \tag{9.37}$$

$\theta_s = \theta_g + 50$, where θ_g is the glass transition temperature and C_1 and C_2 are

https://doi.org/10.1017/CBO9781139171731.010 Published online by Cambridge University Press

constants for the polymer. By the use of (9.37) the variation of hysteresis loss with temperature can be deduced from the variation with frequency. Measurements by Ludema & Tabor (1966) of the variation of rolling friction with temperature at a constant speed were found to follow the variation of hysteresis loss with temperature at a constant frequency.

(c) Surface roughness

It is an everyday experience that resistance to rolling of a wheel is greater on a rough surface than on a smooth one, but this aspect of the subject has received little analytical attention. The surface irregularities influence the rolling friction in two ways. Firstly they intensify the real contact pressure so that some local plastic deformation will occur even if the bulk stress level is within the elastic limit. If the mating surface is hard and smooth the asperities will be deformed plastically on the first traversal but their deformation will become progressively more elastic with repeated traversals. A decreasing rolling resistance with repeated rolling contact has been observed experimentally by Halling (1959). The second way in which roughness influences resistance is through the energy expended in surmounting the irregularities. It is significant with hard rough surfaces at light loads. The centre of mass of the roller moves up and down in its forward motion which is therefore unsteady. Measurements of the resistance force by Drutowski (1959) showed very large, high frequency fluctuations: energy is dissipated in the rapid succession of small impacts between the surface irregularities. It is the equivalent on a small scale of a wagon wheel rolling on a cobbled street. Because the dissipation is by impact the resistance from this cause increases with the rolling speed.